Electronic Supplementary Information (ESI) for Chemical Communications. This journal is (c) The Royal Society of Chemistry 2024.
Electronic Supplementary Information (ESI)

Rationally engineering a binary $SnS_{0.5}Se_{0.5}$/carbon nest-coated Si nanosphere for high-performance lithium-ion battery anode

Hui Zhang[a], Kehao Tao[b,c], Xiangbing Zeng[d], Chengbing Chen[d], Yajun Zhu[a,e], Tianli Han[a], Jinjin Li[b,c,*], and Jinyun Liu[a,*]

Experimental

Materials and reagents

Si particles (diameter: 40-100 nm), $SnCl_2 \cdot 2H_2O$, absolute ethanol, N, N-dimethylformamide (DMF), selenium powders, sulfur powders, and 1,3,5-terephthalic acid were obtained from Aladdin. All chemicals were used directly without further purification.

Preparation of Si-Sn metal-organic frameworks (MOFs) precursor

In a typical process, a solution A composing of 0.5815 g of $SnCl_2 \cdot 2H_2O$, 0.4280 g of 1,3,5-terephthalic acid, 12 mL absolute ethanol and 48 mL DMF was prepared in a 100 mL beaker after magnetically stirring by an agitator for 10 min. Then, 0.1 g of Si as core material was added to 100 mL of beaker containing 12 mL of absolute ethanol, and ultrasonicated for 30 min to obtain solution B. Solution A and B were mixed and stirred for 10 min. The obtained solution was transferred to a 50 mL polytetrafluoroethylene reaction autoclave in an oven and heated at 150 °C for 12 h. After cooling down to room temperature, the sample with MOFs coating on Si was washed several times with deionized water, and dried at 60 °C for 12 h.

Preparation of Si@$SnS_{0.5}Se_{0.5}$/C

The Si-Sn precursor and sulfur powders were putted in a quartz boat with mass ratio of 1:3, and calcined at 500 °C for 4 h with a heat rate of 3 °C min^{-1} under Ar gas flow. After calcination, the sample and selenium powders were putted in a quartz boat with mass ratio of 1:1, and calcined at 500 °C for 4 h with a heat rate of 2 °C min^{-1} under Ar/H_2 (95%/5%) gas flow. After calcination, the Si@$SnS_{0.5}Se_{0.5}$/C was obtained. For comparison, $SnS_{0.5}Se_{0.5}$/C was also prepared through similar process without adding Si particles.

Characterization

The sample was characterized by using an X-ray diffractometer (XRD, SMART APEX II Brook, copper target). The morphology was observed by field emission scanning electron microscope (SEM, Hitachi S-8100), and transmission electron microscope (TEM, HT-7700, TecnaiG220S-Twin). A high-resolution TEM (HRTEM) was used to observe the lattice fringes. Energy dispersive X-ray spectroscopy (EDS) was employed for elemental mapping and studying the elemental distribution. X-ray photoelectron spectroscopy (XPS, EscalAB 250) and Raman spectroscopy (Renishaw in Via) were used for characterization. In order to characterize the carbon matrix, Raman spectroscopy (Renishaw in Via) was used. Prior to the Brunauer-Emmett-Teller (BET) test, the sample was degassed at 120 °C for 12 h in vacuum to remove water adsorbed on the surface, and then physical adsorption isotherms (adsorption-desorption branch) were recorded using a specific surface area tester (ASAP Micromeritics Tristar 2460).

Electrochemical tests

The active materials (75 wt%), acetylene black (15 wt%) and polyvinylidene fluoride (PVDF, 10 wt%) were mixed in a ratio of 7.5:1.5:1. The n-methyl-pyrrolidone (NMP) was used as diluent to disperse the mixture. Evenly-mixed slurry was coated on a Cu foil with a thickness of 9 μm, dried in a vacuum oven at 80 °C for 24 h, and cut into 1.2 mm-diameter discs. The mass loading of the anode was about 1.2 mg cm^{-2}. The electrolyte consisted of 1 mol L^{-1} $LiPF_6$ in ethylene carbonate (EC), dimethyl carbonate (DMC) and ethyl methyl-carbonate (EMC) with volume ratio of 2:6:2. The process of assembling was in an argon-filled glove box. The galvanostatic charge-discharge (GCD) was tested on Neware Battery system. Cyclic voltammetry (CV, 0.1 mV s^{-1} of sweep rate over the range of 0.01-3 V) and electrochemical impedance spectroscopy (EIS) test were performed an electrochemical workstation (CHI 660E). The time-voltage relationship was obtained by using galvanostatic intermittent titration technique (GITT) on a battery tester (Neware CT4008). At a current density of 0.2 A g^{-1}, the cell was charged/discharged to the preset potential in 10 min and stood by 2 h before going to next potential.

First-principle calculations

General ab initio method has been used to study the stress-strain and tensile strain relationships of Li-Si systems. In this work, the focus was not on elastic properties, but on the

mechanical behavior of the lithium-germanium system, where the tensile strength was determined by elastic instability and can be evaluated by the relationship between strain and stress along the high symmetry axis. The equilibrium state of the Li-Si system can be obtained by optimizing six kinds of lithium-germanium structures (Li, Si, LiSi, Li_7Si_2, Li_9Si_4, $Li_{11}Si_6$). First-principles calculations for structural optimization were performed in the Vienna ab initio simulation package (VASP) using density functional theory (DFT) with Perdew-Burke-Ernzerhof (PBE) exchange correlation functional. The Projector Augmented Wave (PAW) potentials were calculated by the generalized gradient approximation function for Li and Si. The kinetic energy cutoff for a plane wave basis set was 500 eV and emerged the excellent convergence of the total energy. Moreover, all force on atoms were converged to less than 10^{-5} eV/ Å.

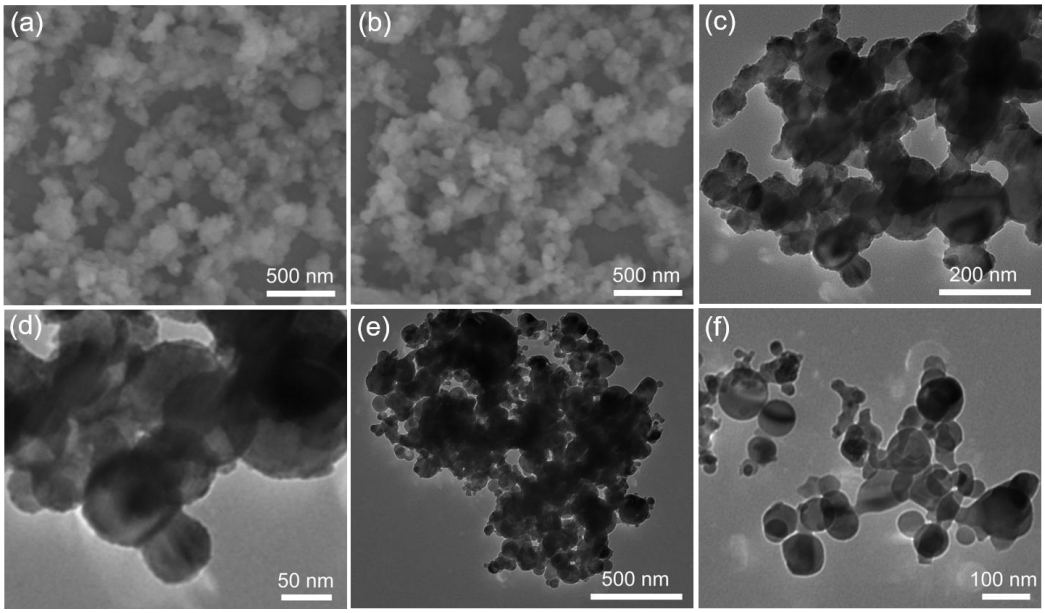

Fig. S1 (a,b) SEM and (c,d) TEM morphologies of Si-Sn MOFs precursor. (e,f) TEM images of the bare Si.

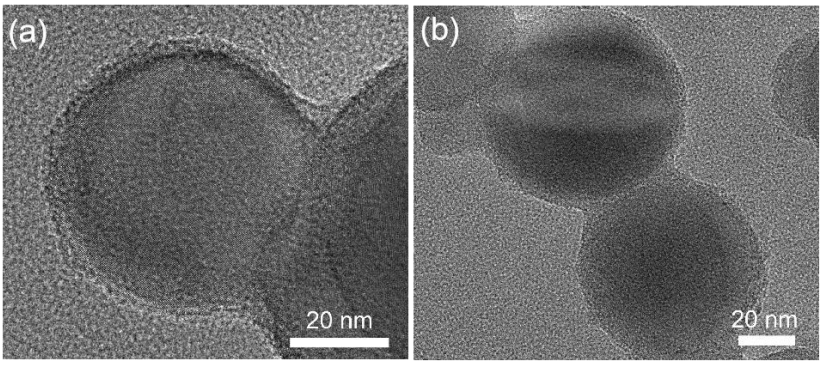

Fig. S2 (a,b) TEM images of $Si@SnS_{0.5}Se_{0.5}/C$.

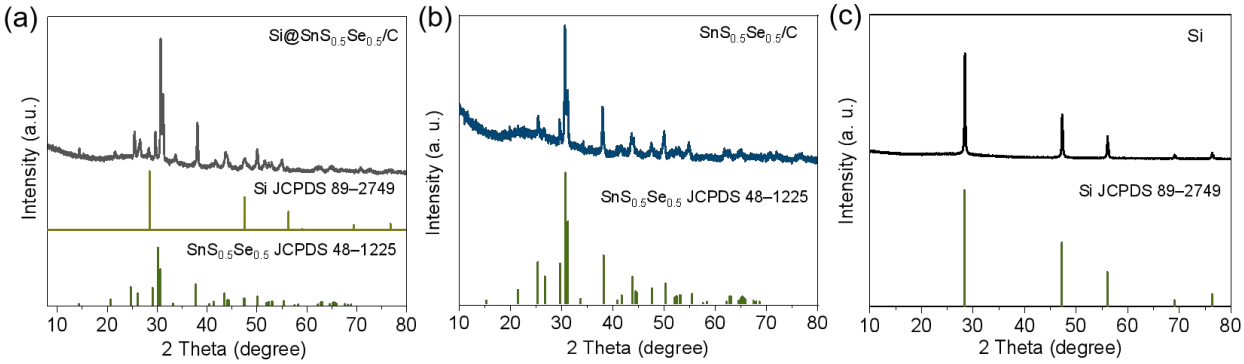

Fig. S3 XRD patterns of (a) $Si@SnS_{0.5}Se_{0.5}/C$, (b) $SnS_{0.5}Se_{0.5}/C$, and (c) Si.

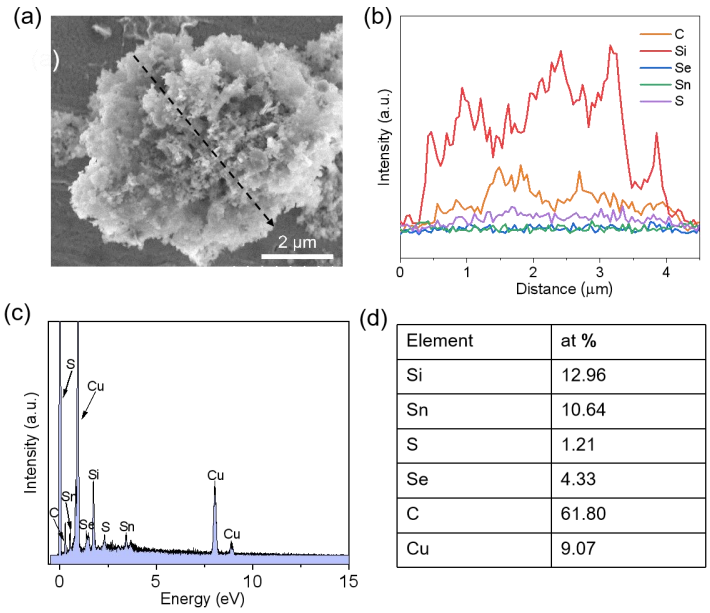

Element	at %
Si	12.96
Sn	10.64
S	1.21
Se	4.33
C	61.80
Cu	9.07

Fig. S4 (a) SEM image, (b) line-scanning curves, (c) EDS spectrum and (d) elemental contents of Si@$SnS_{0.5}Se_{0.5}$/C.

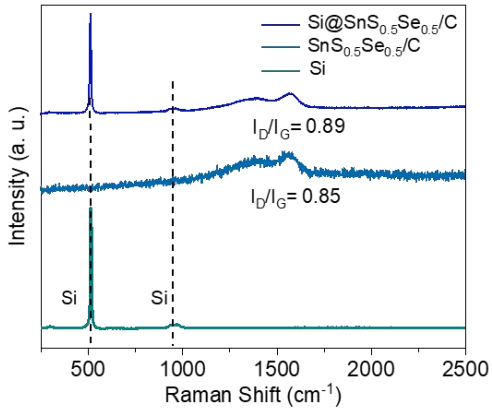

Fig. S5 Raman spectra of Si@$SnS_{0.5}Se_{0.5}$/C, $SnS_{0.5}Se_{0.5}$/C, and Si.

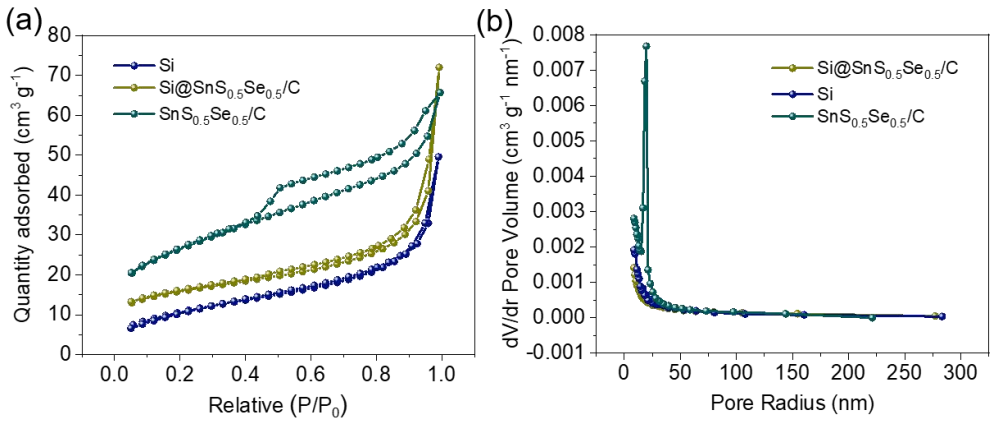

Fig. S6 (a) The N_2 adsorption-desorption isotherms and (b) pore-size distribution of Si@$SnS_{0.5}Se_{0.5}$/C, $SnS_{0.5}Se_{0.5}$/C, and Si.

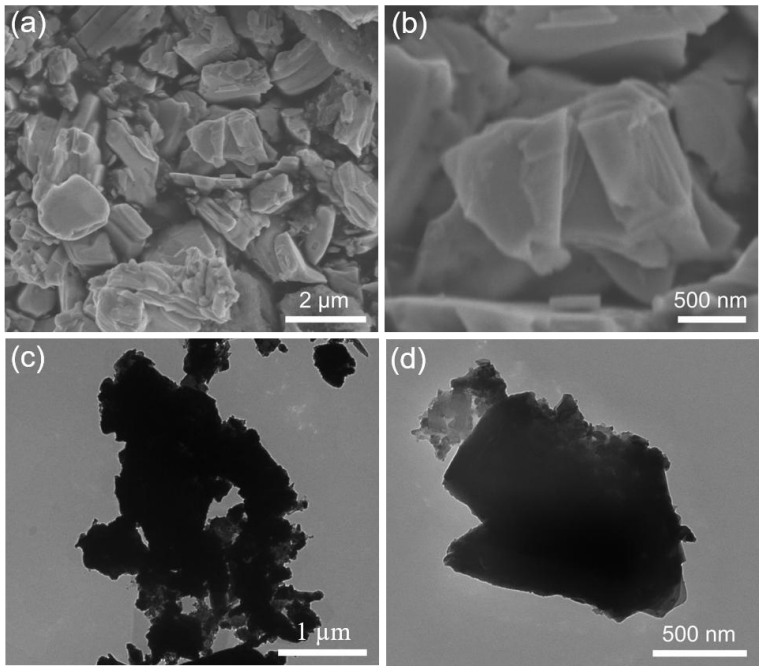

Fig. S7 (a,b) SEM and (c,d) TEM images of $SnS_{0.5}Se_{0.5}$/C.

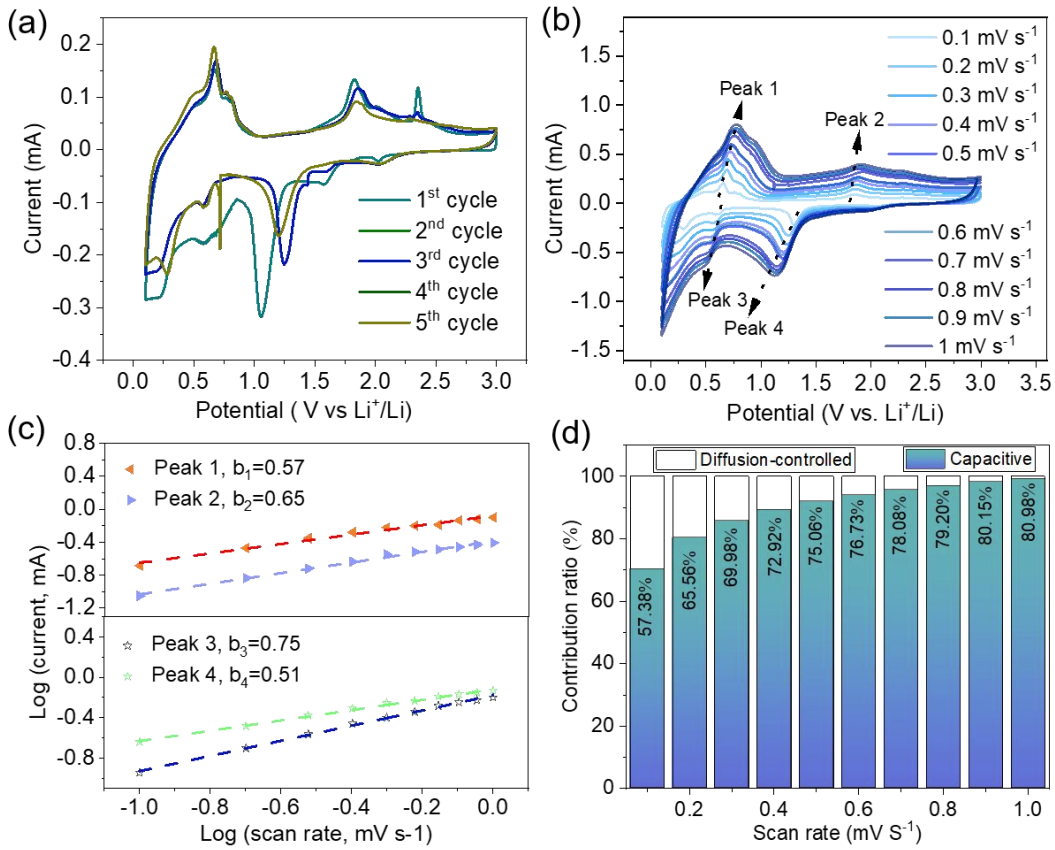

Fig. S8 (a) CV profiles of $SnS_{0.5}Se_{0.5}$/C anode at 0.1 mV s^{-1}. (b) CV curves at 0.1 to 1.0 mV s^{-1}. (c) The log (*i*) vs. log (*v*) of oxidization and reduction peaks, and (d) ratio of contributions.

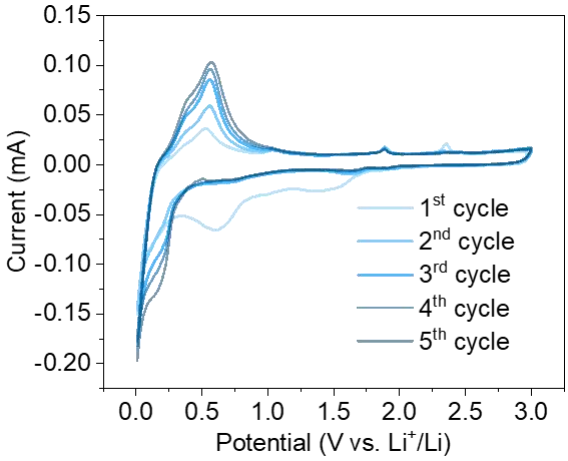

Fig. S9 CV profiles of Si anode scanning at 0.1 mV s^{-1}.

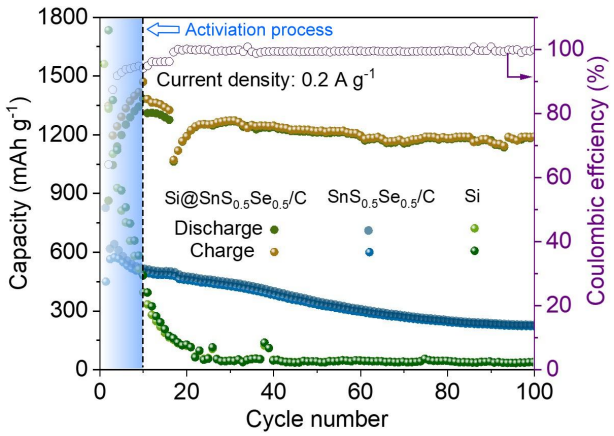

Fig. S10 Cycling performance of Si@$SnS_{0.5}Se_{0.5}$/C, $SnS_{0.5}Se_{0.5}$/C, Si anodes at 0.2 A g^{-1}. The anodes were pre-cycled 10 cycles at 0.1 A g^{-1} for activation.

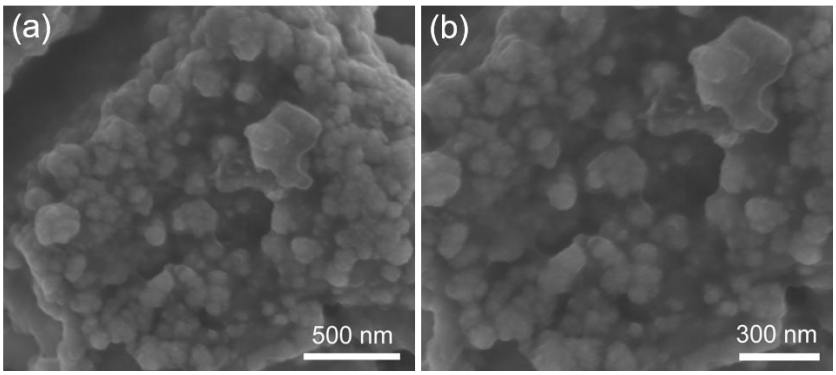

Fig. S11 (a,b) SEM images of Si@$SnS_{0.5}Se_{0.5}$/C after cycling 100 times at 0.2 A g^{-1}.

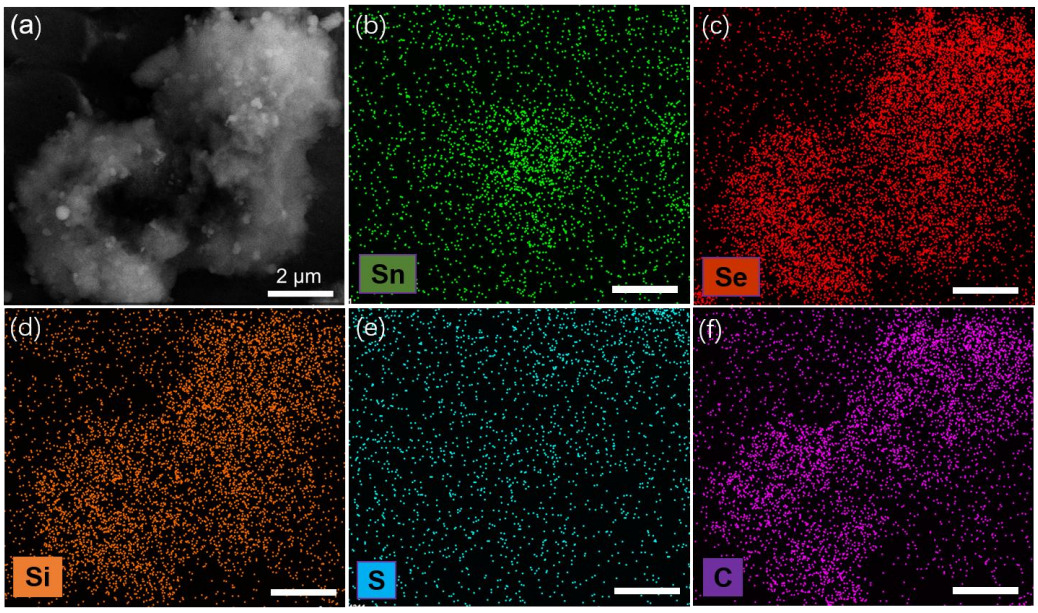

Fig. S12 (a) SEM and (b-f) mapping images of the Si@$SnS_{0.5}Se_{0.5}$/C after cycling 100 times at 0.2 A g^{-1}.

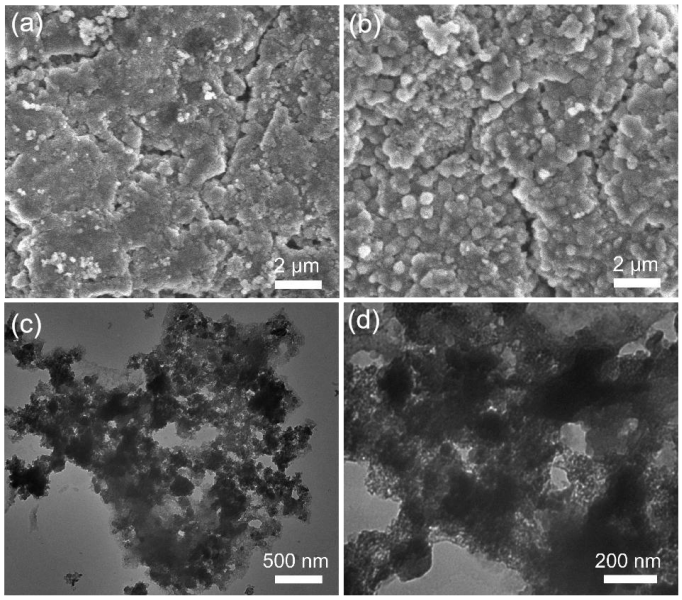

Fig. S13 (a,b) SEM and (c,d) TEM images of $SnS_{0.5}Se_{0.5}$/C after cycling 100 times at 0.2 A g^{-1}.

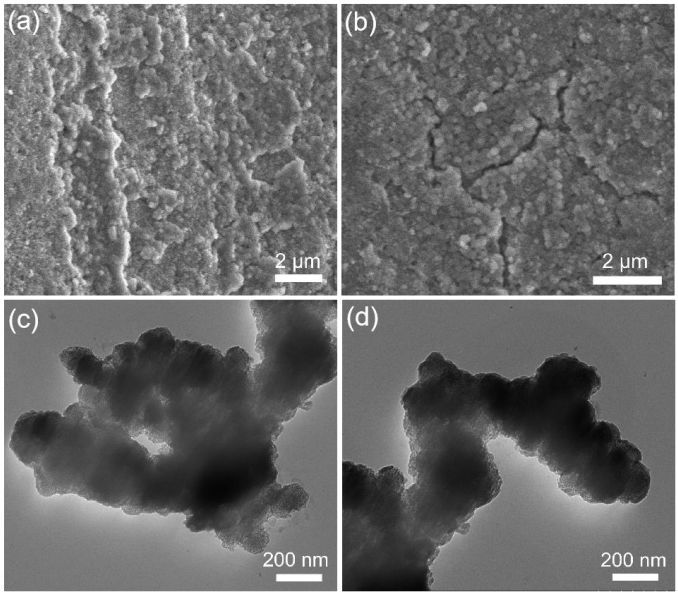

Fig. S14 (a,b) SEM and (c,d) TEM images of pure Si after cycling 100 times at 0.2 A g^{-1}.

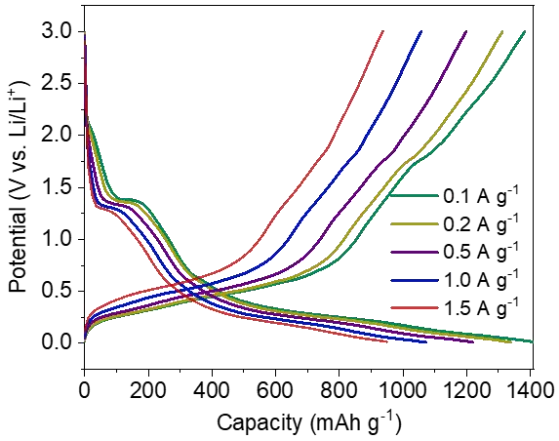

Fig. S15 Galvanostatic discharge-charge curves of Si@$SnS_{0.5}Se_{0.5}$/C at different current densities from 0.1-1.5 A g^{-1}.

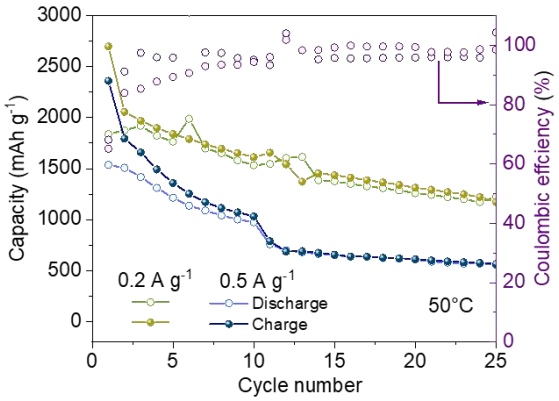

Fig. S16 Cycling performance of Si@$SnS_{0.5}Se_{0.5}$/C anode under 50°C at 0.2 and 0.5 A g^{-1}.

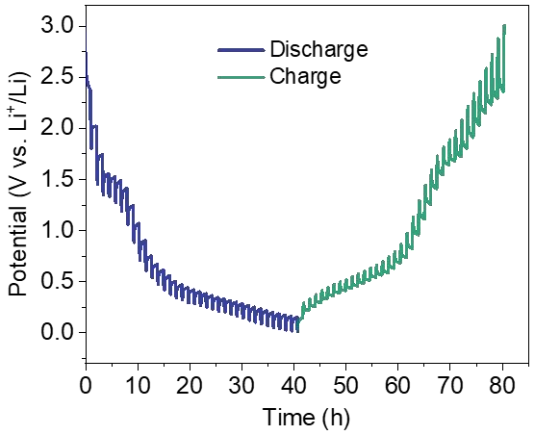

Fig. S17 GITT time-potential distributions of Si@$SnS_{0.5}Se_{0.5}$/C.

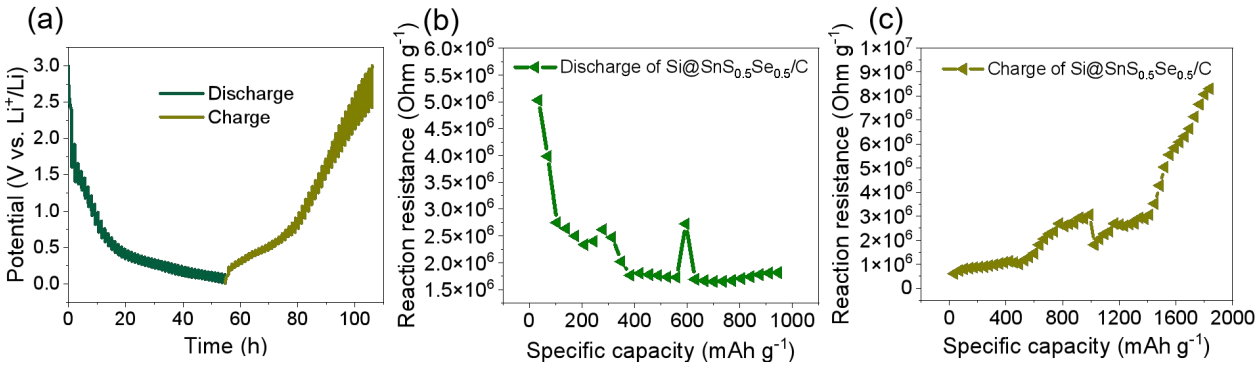

Fig. S18 (a) GITT time-potential distributions of Si@$SnS_{0.5}Se_{0.5}$/C at 50 °C. *In situ* reaction impedances of Si@$SnS_{0.5}Se_{0.5}$/C during (b) discharge and (c) charge at 50 °C.

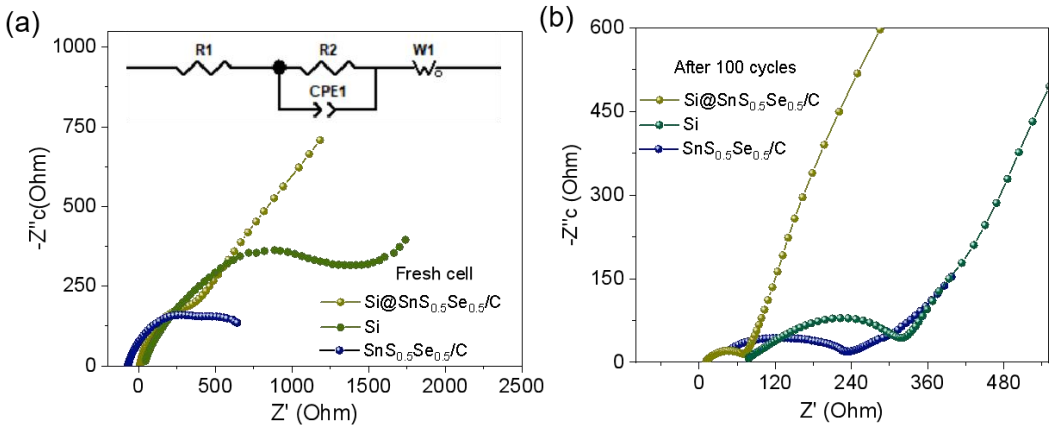

Fig. S19 EIS spectra of Si@$SnS_{0.5}Se_{0.5}$/C, $SnS_{0.5}Se_{0.5}$/C and Si (a) before and (b) after 100 cycles at 0.2 A g^{-1}. The insert displays the equivalent circuits.

Table S1. Comparison on the electrochemical performance of some Li-ion battery anodes.

Anode materials	Current density (A g^{-1})	Capacity (mAh g^{-1})	Cycle number	Ref.
Si@$SnS_{0.5}Se_{0.5}$/C	0.1	1318	50	This work
	0.2	1174	100	
	0.5	887	150	
Si	0.1	1270	25	[1]
Si@mesocarbon-microbeads	0.2	421	200	[2]
Si@C	0.1	1038	50	[3]
Si@Fe_3O_4	0.2	697	100	[4]
Si-Ni-C	0.2	524	100	[5]
Si@C	0.1	713	50	[6]
SnS_2	0.5	80	450	[7]
SnSe	0.1	100	300	[8]

References

(1) D. Lou, S. Y. Chen, S. Langrud, A. A. Razzaq, M. Y. Mao, H. Younes, W. B. Xing and T. Lin, *Appl. Sci.*, 2022, **12**, 10926.

(2) J. T. Du, J. K. M, Z. T. Liu, W. C. Wang, H. N. Jia, M. X. Zhang and Y. Nie, *Mater. Lett.*, 2022, **315**, 131921.

(3) X. Y. Shen, M. Chen, Z. K. Qiao, W. D. Wang, Y. C. F, J. Chen and C. J. Tang, *Mater. Res. Express*, 2019, **6**, 115538.

(4) Y. X. Chen, Y. J. Yan, X. l. Liu, X. Y. Wu, J. Zhou and Z. F. Wang, *Nanomaterials*, 2020, **10**, 2331.

(5) Q. R. Liu, Y. Gao, P. G. He, C. Yan, Y. Gao, J. Z. Gao, H. B. Lu and Z. B. Yang, *Mater. Lett.*, 2018, **231**, 205-208.

(6) Y. H. He, Y. F. Lin, J. W. Jiang, D.R. Yang, N. D, X. Q. He, J. G. Ren, P. He, C. L. Pang, C. M. Xiao, Y. F. Chen and L. Bao, *Ionics*, 2019, **25**, 5809-5818.

(7) Y. H. Xie, M. P. Fan, T. Shen, Q. W. Liu and Y. Chen, *Mater. Technol*., 2022, **31**, 646-652.

(8) Y. P. Chen, Q. L. Yang, P. B. Wu, T. X. Xu, J. Wang and Y. J. Li, *ACS Appl. Nano Mater.*, 2021, **4**, 13010-13017.